Effects of Catalyst Acidity and HZSM-5 Channel Volume on the Catalytic Cracking of Poly(ethylene)

RONG LIN and ROBERT L. WHITE*

Department of Chemistry and Biochemistry, University of Oklahoma, Norman, Oklahoma 73019

SYNOPSIS

The effects of catalyst acidity and the restricted reaction volume afforded by the HZSM-5 zeolite structure on the volatile cracking products derived from poly(ethylene) are investigated. The effectiveness of silica-alumina, HZSM-5, and sulfated zirconia acid catalysts for poly(ethylene) cracking are compared. When high catalyst to polymer ratios are employed and volatile products are rapidly removed during cracking, the most abundant volatile products generated by poly(ethylene) cracking are propene and isoalkenes. The relative amount of propene produced and the temperatures corresponding to the maximum rate of volatile hydrocarbon production are found to be related to catalyst acidity. The restricted volume inside HZSM-5 channels facilitates oligomerization and the production of small alkyl aromatics. © 1995 John Wiley & Sons, Inc.

INTRODUCTION

It is undesirable to dispose of waste plastics by landfilling because of their poor biodegradability. As alternatives, methods for recycling plastic waste have been established, and new recycling approaches are being developed. The American Society for Testing and Materials (ASTM) has defined four different types of plastics recycling methods.[1] Primary recycling can be applied to waste plastics that are free of impurities. In these methods, waste plastics are used in plastics manufacturing processes in the same manner that virgin plastics are used. When waste plastics are comprised of a single homopolymer but contain some impurities, secondary recycling can be employed. In secondary recycling, the plastics industry uses waste plastics to produce products that have less demanding performance characteristics (e.g., plastic bags) than those produced by primary recycling techniques. In tertiary recycling, waste plastics are converted into useful chemicals. Plastic waste containing multiple homopolymers and significant impurities can be treated by tertiary recycling techniques. Waste-to-energy (WTE) tech-

niques constitute quaternary plastics recycling. In this type of recycling, plastic waste is burned to produce energy.

For any recycling scheme to be economically viable, the costs of collecting and sorting waste and for reclaiming products from waste must be recovered. Recent studies supported by the Packaging Research Foundation have shown that, based on the current price of oil, these costs cannot presently be recovered for tertiary plastic waste recycling methods.[2] However, future increases in landfilling costs, coupled with lower collecting and sorting costs, may make tertiary plastic waste recycling economically viable in the near future.

Large-scale plastic waste tertiary recycling will require efficient catalytic cracking of waste polymers. The development of waste polymer cracking processes will require detailed knowledge of the relationship between catalyst properties and cracking product distributions. Previous studies of the catalytic cracking of poly(ethylene), which constitutes about 60% of the total plastic waste volume,[3] have shown that the molecular weight range of volatile products generated by heating this polymer can be greatly reduced by the presence of acid catalysts.[4-13] Studies of the effects of catalysts on the thermal degradation of poly(ethylene) have been performed by: contacting melted polymer with catalyst in fixed

bed reactors,[4,5] heating mixtures of polymer and catalyst powders in reaction vessels,[6–8,10,11] and passing the products of poly(ethylene) pyrolysis through reactors containing cracking catalysts.[12,13] For those studies in which the polymer was placed in direct contact with catalysts, it has been reported that the catalyst-to-polymer ratio has an effect on the relative abundance of the volatile products.[10]

In order to compare the polymer cracking properties of different catalysts, it is preferable to examine the effects of catalysts without complications due to reactions of primary cracking products with polymer residue. Secondary reactions can be minimized by limiting the contact between primary volatile products and the catalyst/polymer mixture. This can be accomplished by using high catalyst-to-polymer ratios and providing efficient and rapid removal of volatile products. In this article, thermal analysis results obtained from samples prepared by coating silica-alumina, HZSM-5, and sulfated zirconia catalysts with thin layers of poly(ethylene) are compared. Catalytic activity and ammonia TPD studies have shown that HZSM-5 is a significantly stronger acid catalyst than amorphous silica-alumina.[14] Sulfated zirconia is an even stronger acid catalyst than HZSM-5[15]. In fact, sulfated zirconia has been called a solid superacid.[16] By comparing the thermal properties of poly(ethylene) in contact with these three catalysts, the influence of catalyst acidity and HZSM-5 channel structure on volatile catalytic cracking product distributions can be assessed.

EXPERIMENTAL

Samples examined in this study were: neat poly(ethylene) and poly(ethylene) coated on silica-alumina, HZSM-5, and sulfated zirconia cracking catalysts [10–15% (wt/wt)]. Poly(ethylene) powder (M_w = 80,000) was purchased from Aldrich Chemical Company (Milwaukee, WI). The silica-alumina catalyst was prepared by following procedures described in the literature.[17] The silica-alumina catalyst contained 9.5% by weight alumina and had a surface area of 211 m^2/g. The HZSM-5 catalyst was obtained from Mobil Oil Corp. (Paulsboro, NJ) and was characterized by a 355 m^2/g surface area and a 1.5% alumina content. The sulfated zirconia catalyst was prepared by following procedures described in the literature.[18] The sulfated zirconia catalyst had a surface area of 157 m^2/g and contained 9% by weight sulfate. Poly(ethylene)/catalyst samples were prepared by dissolving appropriate

amounts of poly(ethylene) in decane at about 80°C. After the addition of the catalyst, the mixtures were rotoevaporated until solvents were removed. The remaining polymer coated catalyst samples were dried for several hours at 120°C.

TGA-MS measurements were made by connecting the gas outlet of a Du Pont (Wilmington, DE) Model 951 TGA analyzer to a Hewlett Packard (Palo Alto, CA) 5985 quadrupole mass spectrometer by using a Scientific Glass Engineering Inc. (Austin, TX) MCVT-1-50 variable splitting valve. The TGA-MS interface was maintained at 200°C during measurements. Helium flow through the TGA during measurements was at a rate of 50 mL/min. Poly(ethylene)/catalyst samples were heated from 50°C to 700°C at rates of 1, 10, 25, and 50°C/min. Mass spectra were acquired by using 70 eV electron bombardment ionization and scanning from m/z 10 to m/z 500 at a rate sufficient to record at least one signal-averaged spectrum for each 10°C temperature increment. The mass spectrometer ion source pressure was maintained at 5 × 10^{-6} Torr for the 50°C/min and 25°C/min sample heating rates and 2 × 10^{-5} Torr for the 10°C/min and 1°C/min sample heating rates.

Pyrolysis-GC/MS experiments were performed by using a microfurnace pyrolyzer GC injector built in our laboratory and described elsewhere.[19] Separations were achieved by using a Hewlett Packard 5890A capillary gas chromatograph equipped with a 25 m Hewlett Packard Ultra-1 column (0.52 μm film thickness) in series with a 30 m DB-5 column (0.25 μm film thickness). The gas chromatograph oven temperature program consisted of a 2-min isothermal period at −50°C followed by a 5°C/min ramp to 40°C and a 10°C/min ramp from 40 to 300°C. About 2 mg samples were put into glass capillary tubes for pyrolysis experiments. Helium was employed as the carrier gas at a flow rate of 0.8 mL/min. Mass spectra were acquired by a Hewlett Packard 5988 quadrupole mass spectrometer scanning from m/z 10 to 250 at a rate of 20 spectra/min for poly(ethylene)/catalyst samples and from m/z 10 to 500 at a rate of 10 spectra/min for neat poly(ethylene). Mass spectral library searches employed a 36,218 spectra NBS mass spectral library.

RESULTS

Poly(ethylene) catalytic cracking mechanisms for the three catalysts were compared by using TGA–MS to correlate the polymer weight loss with production of specific classes of volatile hydrocarbons.
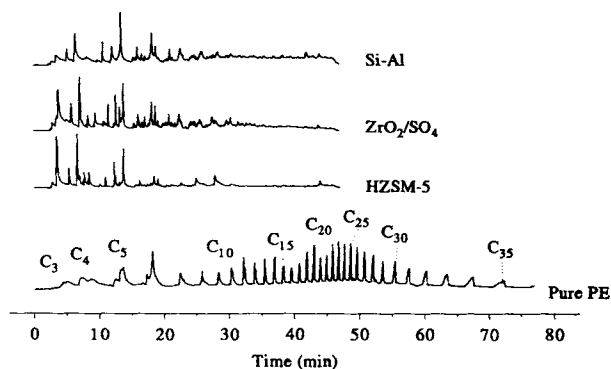
Figure 1 Pyrolysis-GC/MS chromatograms for neat poly(ethylene) and poly(ethylene)/catalyst samples obtained at 500°C.

Because different hydrocarbon products were simultaneously evolved during TGA–MS analysis, it was necessary to identify mass spectral ions that were hydrocarbon class specific. This was achieved by using pyrolysis-GC/MS. Pyrolysis-GC/MS experiments were performed at 400, 500, and 600°C for each of the poly(ethylene)/catalyst samples. GC/MS selected ion chromatograms revealed that hydrocarbon molecular ion intensities could be used as a semiquantitative means of representing classes (e.g., alkanes, alkenes, and aromatics) by carbon number. For example, m/z 56 ion intensity was found to be representative of butenes, whereas m/z 58 was found to indicate the presence of butanes. Unfortunately, temperature profiles for ethylene and propane could not be generated from TGA–MS mass spectra because the molecular ions for these species (m/z 28 and m/z 44) could not be distinguished from background ion signals due to CO and CO_2.

Figure 1 illustrates the dramatic effect that the catalysts had on the thermal degradation of poly(ethylene). All four chromatograms shown in Figure 1 were obtained by using the same separation conditions and they are plotted on the same time axis. The chromatogram shown at the bottom of Figure 1, which represents the volatile products from the thermal degradation of neat poly(ethylene) at 500°C, contains numerous elutions, many of which correspond to relatively high molecular weight species. In contrast, pyrolysis-GC/MS chromatograms obtained when catalysts were present exhibit few elutions after 30 min (e.g., $> C_{10}$). Thus, the effect of the catalyst was to restrict the molecular weight range of volatile hydrocarbon products, leading primarily to the production of low molecular weight species. However, as illustrated by chromatogram differences shown in Figure 1, the volatile product

distributions for the three poly(ethylene)/catalyst samples were quite different.

Pyrolysis-GC/MS mass spectral library searches for neat poly(ethylene) elutions indicated that the primary products were 1-alkenes. Many of the 1-alkene chromatographic peaks were accompanied by two smaller peaks, one eluting prior to the 1-alkene and the other eluting after. The early eluting peak was identified as an alkadiene, whereas the late eluting peak was identified as an alkane. Mass spectra corresponding to these additional peaks indicated that these species had the same number of carbon atoms as the 1-alkene. These findings are consistent with previously published results of poly(ethylene) pyrolysis.[6,20]

Pyrolysis-GC/MS results obtained for the poly(ethylene)/catalyst samples at 400, 500, and 600°C were compared to investigate the temperature dependence of volatile products. Major products consisted of alkenes, alkanes, and aromatics. Alkadienes were not detected in significant quantities for any of the poly(ethylene)/catalyst samples. Table I contains the volatile product distributions derived from chromatograms obtained at 500 and 600°C microfurnace temperatures for samples comprised of poly(ethylene) coated on the silica-alumina catalyst. No information regarding catalytic

Table I Pyrolysis Products for the Poly(ethylene)/Silica-Alumina Sample

Class	Relative Abundance (%)[a]	
	500°C	600°C
Propene	10.83	9.76
C_4-Alkanes	3.87	2.42
C_4-Alkenes	14.15	14.37
C_5-Alkanes	1.92	1.66
C_5-Alkenes	15.36	15.07
C_6-Alkanes	4.71	2.00
C_6-Alkenes	17.52	16.97
C_6-Alkadienes	0.64	
C_7-Alkanes	0.35	1.68
C_7-Alkenes	9.23	9.00
C_8-Alkanes	0.14	
C_8-Alkenes	3.02	4.13
C_8-Alkadienes	1.06	
C_9-Alkenes	2.60	3.57
C_{10}-Alkenes	2.70	2.08
C_{11}-Alkenes	1.52	4.05
C_{12}-Alkenes	0.65	2.26
C_{13}-Alkenes	0.49	1.34
C_{14}-Alkenes	0.72	1.23
C_{15}-Alkenes	0.51	0.23

[a] Percentage of integrated total ion current.

Table II Pyrolysis Products for the Poly(ethylene)/HZSM-5 Sample

Class	Relative Abundance (%)[a]		
	400°C	500°C	600°C
Ethylene	1.06	3.00	5.54
Propane	0.09	0.03	0.63
Propene	23.78	22.24	19.53
C_4-Alkanes	11.46	7.12	4.92
C_4-Alkenes	22.51	20.35	21.77
C_5-Alkanes	5.12	4.65	5.95
C_5-Alkenes	8.51	11.04	12.77
C_6-Alkanes	2.09	1.96	1.96
C_6-Alkenes	5.71	5.71	8.75
C_7-Alkanes	1.17	1.82	1.47
C_7-Alkenes	0.39	0.40	0.33
Aromatics	9.17	18.38	7.48

[a] Percentage of integrated total ion current.

Table III Pyrolysis Products for the Poly(ethylene)/Sulfated Zirconia Sample

Class	Relative Abundance (%)[a]		
	400°C	500°C	600°C
CO	0.42	0.12	0.40
CO_2	2.12	3.88	23.44
Propane	3.28		
Propene	6.18	11.03	10.83
C_4-Alkanes	7.67	2.79	2.01
C_4-Alkenes	18.63	14.59	10.80
C_5-Alkanes	7.98	1.58	0.67
C_5-Alkenes	12.76	10.76	11.19
C_6-Alkanes	6.35	2.37	1.78
C_6-Alkenes	8.77	12.11	9.86
C_6-Alkadienes		1.14	
C_7-Alkanes	3.36	0.48	0.39
C_7-Alkenes	5.73	8.94	12.17
C_7-Alkadienes	0.15		
C_8-Alkanes	2.11		
C_8-Alkenes	2.91	4.99	4.06
C_8-Alkadienes	3.34		
C_9-Alkenes	3.05	3.29	4.56
C_{10}-Alkenes	3.33	2.52	3.94
C_{11}-Alkenes	0.71	1.71	0.08
C_{12}-Alkenes		1.27	
C_{13}-Alkenes		0.34	

[a] Percentage of integrated total ion current.

cracking processes at 400°C was obtained for the poly(ethylene)/silica-alumina sample. Chromatograms obtained at this temperature contained broad, overlapping peaks, indicating that volatile product formation processes in the microfurnace were too slow at this temperature. At 500°C, 92% of the volatile hydrocarbon products detected were in the C_3 to C_{15} range. At 600°C, a slight reduction in the fraction of low molecular weight products and an increase in the fraction of high molecular weight alkenes compared to the product distribution obtained at 500°C (C_{11} and C_{12} in particular) suggests that the contributions to volatile products from thermal cracking processes were greater at the higher temperature. Pyrolysis-GC/MS results for the poly(ethylene)/zeolite sample are contained in Table II. Seventy-eight percent of the volatile products at 500°C were assigned to C_2–C_7 alkenes and alkanes, and 18% of the volatile products were found to be aromatic. The fraction of ethylene produced increased with microfurnace temperature, whereas the fraction of C_4 alkanes detected decreased substantially. Perhaps the most significant volatile product distribution change with temperature involved the fraction of aromatics formed. The proportion of aromatics formed at 500°C was about twice that detected at 400°C but the proportion of aromatics detected at 600°C was less than that found at 400°C, indicating that there was an optimum temperature for aromatization. Pyrolysis-GC/MS product distributions for the poly(ethylene)/sulfated zirconia catalyst are contained in Table III. Eighty percent of the volatile products at 500°C were C_3–C_{13} alkenes and alkanes. The fraction of volatile

products due to C_3–C_8 alkanes and C_4 alkenes significantly decreased with increasing microfurnace temperature. A dramatic increase in the fraction of CO_2 detected was observed at 600°C.

The TGA–MS weight loss curves for neat poly(ethylene) and the poly(ethylene)/catalyst samples are shown in Figure 2. The left y-axis in Figure 2 refers to the neat poly(ethylene) weight
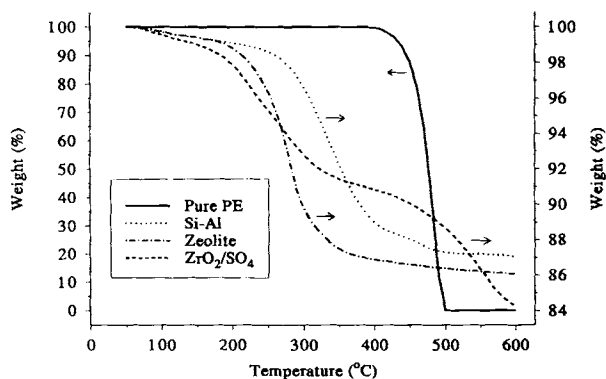

Figure 2 TGA–MS weight loss curves for neat poly(ethylene) and poly(ethylene)/catalyst samples obtained by heating samples at a rate of 10°C/min.
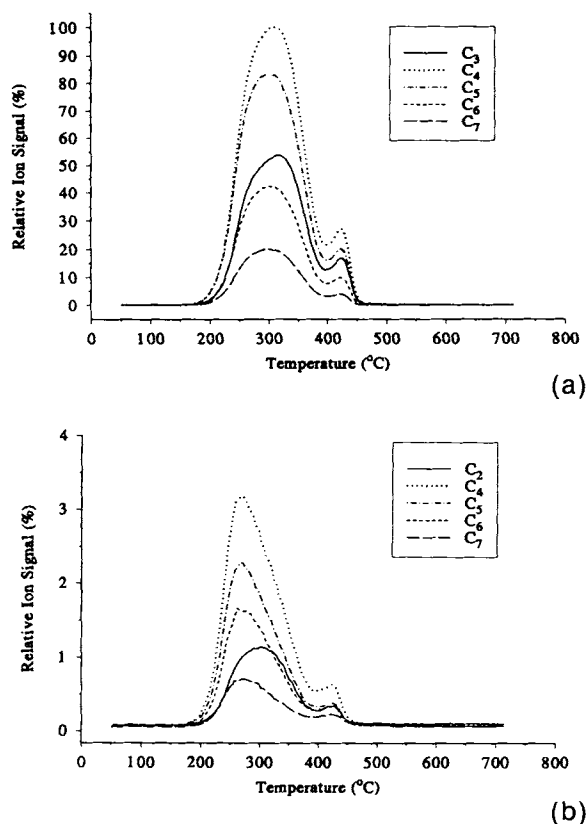
(a)

(b)

Figure 3 Class-specific ion signal temperature profiles derived from TGA–MS analysis of the poly(ethylene)/ silica-alumina sample for (a) alkenes and (b) alkanes.

loss curve (solid line), and the right y-axis corresponds to the poly(ethylene)/catalyst samples. Weight loss due to catalytic cracking began about 200°C lower than weight loss attributed to thermal cracking. The order in which weight loss began as poly(ethylene)/catalyst samples were heated was found to be in the order of decreasing catalyst acidity: sulfated zirconia > HZSM-5 > silica-alumina. The weight loss curve for the poly(ethylene)/silica-alumina sample consisted of two steps. The first step began at about 250°C and exhibited a 12% weight loss. The second step, which began above 400°C, constituted approximately a 1% weight loss. The weight loss curve for the poly(ethylene)/ HZSM-5 sample appeared to be a single step corresponding to about 14% weight loss that began at 200°C and ended near 350°C. The poly(ethylene)/ sulfated zirconia weight loss curve exhibited two steps of comparable weight loss. The first step began near 200°C, ended at about 350°C, and corresponded to about 8% weight loss. The second weight loss step was not complete by 600°C. It began at 350°C and constituted about 7% weight loss by 600°C.

Figure 3 shows TGA–MS class-specific mass spectral ion intensities as a function of temperature for the poly(ethylene)/silica-alumina catalyst sample. Ion signals shown in Figures 3–7 were scaled so that the maximum ion signal for the most abundant alkene detected during TGA–MS analysis of each poly(ethylene)/catalyst sample was 100%. Alkenes comprised the majority of volatile products for the poly(ethylene)/silica-alumina sample, and alkenes and alkanes evolved in two distinct steps. The first step occurred over the same temperature range as the major weight loss step for this sample (Fig. 2) and constituted most of the volatile products detected by the mass spectrometer. Ion signals characteristic of alkanes exhibited maxima at 275 and 425°C, whereas ion signals representing alkenes exhibited maxima at 320 and 425°C. Class-specific temperature profiles for the poly(ethylene)/HZSM-5 sample are shown in Figure 4. Like the silica-alumina catalyst, the major volatile products formed in the presence of the zeolite catalyst were alkenes and alkenes and alkanes evolved in two steps. Unlike the poly(ethylene)/
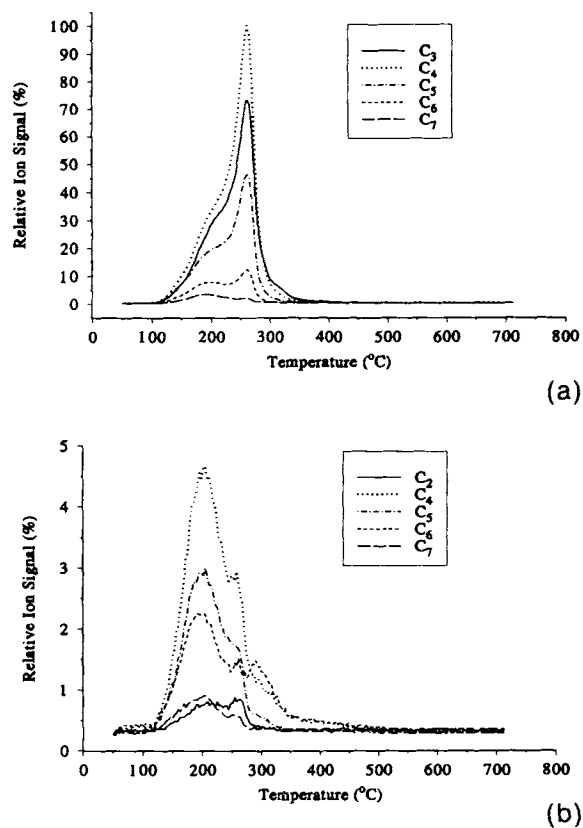

(a)

(b)

Figure 4 Class-specific ion signal temperature profiles derived from TGA–MS analysis of the poly(ethylene)/ HZSM-5 sample for (a) alkenes and (b) alkanes.
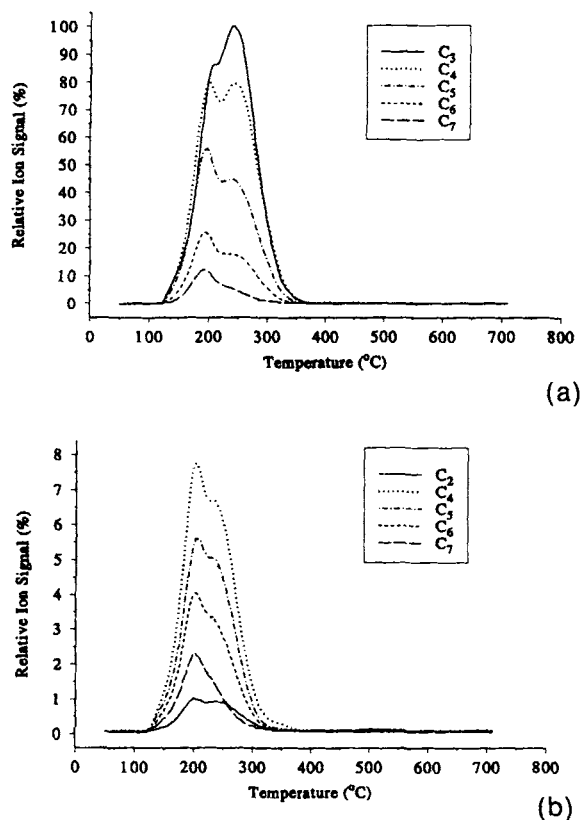
Figure 5   Class-specific ion signal temperature profiles derived from TGA–MS analysis of the poly(ethylene)/sulfated zirconia sample for (a) alkenes and (b) alkanes.

silica-alumina sample, most volatile hydrocarbon products were produced during the second evolution. The maximum rate of alkane formation occurred at 200°C, whereas the maximum rate of alkene formation occurred at 270°C. Compared to the poly(ethylene)/silica-alumina sample, volatile product evolution from the poly(ethylene)/HZSM-5 sample started and ended at lower temperatures. Figure 5 shows ion signal temperature profiles representing TGA–MS evolution of alkenes and alkanes for the poly(ethylene)/sulfated zirconia sample. The start and end temperatures corresponding to volatile product evolution for this sample were similar to those for the poly(ethylene)/HZSM-5 sample. Like the other poly(ethylene)/catalyst samples, two steps were evident in the ion signal temperature profiles. The rate of alkane formation reached a maximum at 200°C, whereas the rate of alkene formation exhibited maxima at 200 and 250°C. Figure 6 contains m/z 91 (i.e., tropylium ion) temperature profiles for the three poly(ethylene)/catalyst samples. The tropylium ion ($C_7H_7^+$) is representative of alkyl

aromatics. As shown in Figure 6, the poly(ethylene)/HZSM-5 sample produced the largest fraction of aromatics and the temperature corresponding to the maximum rate of aromatics production (i.e., 290°C) was higher than the temperature corresponding to the maximum rate of alkene formation.

Compared to neat poly(ethylene), the decrease in the temperatures corresponding to the onset of weight loss for samples containing catalysts may be attributed to lower activation energies for acid catalyzed cracking than for free radical thermal cracking processes. Neat poly(ethylene) and the poly(ethylene)/catalyst samples were subjected to TGA–MS analysis in helium (50 mL/min) with heating rates of 1, 10, 25, and 50°C/min to investigate the effects of catalysts on volatilization and class-specific activation energies. TGA–MS weight loss data obtained by using different heating rates were used to calculate volatilization activation energies by using the method described by Friedman.[21] Class-specific activation energies were calculated from the TGA–MS mass spectral information by using the technique of linear programmed thermal degradation mass spectrometry.[22] Volatilization and class-specific activation energies calculated from TGA–MS data for the three poly(ethylene)/catalyst samples are listed in Tables IV and V. All of the catalysts lowered the activation energy for thermal degradation of poly(ethylene) by at least 20 kcal/mol. As shown by Table V, class-specific activation energies decreased with increasing catalyst acidity. Except for the poly(ethylene)/sulfated zirconia sample, volatilization activation energies calculated from weight loss information were similar to the class-specific activation energies derived from mass
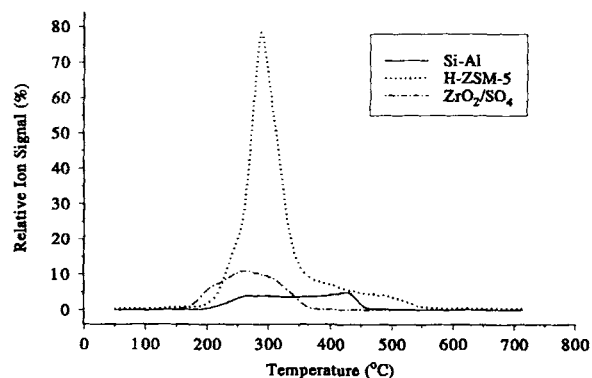

Figure 6   M/z 91 ion signal temperature profiles derived from TGA–MS analysis of the poly(ethylene)/catalyst samples.

**Table IV   TGA-MS Volatilization
Activation Energies**

Sample	E_a (kcal/mol)
PE	58.58 ± 0.78
PE/Silica-Alumina	37.41 ± 2.72
PE/HZSM-5	30.94 ± 1.19
PE/ZrO$_2$/SO$_4$	28.38 ± 2.06

spectral data. The reason that the volatilization activation energy calculated for the poly(ethylene)/ sulfated zirconia was significantly different from class-specific activation energies may have been that, unlike the other polymer/catalyst samples, the two hydrocarbon cracking steps for this sample were of comparable importance. Thus, the assumption that TGA weight loss could be considered to be a single decomposition process, which was apparently valid for the other samples, was not valid for this sample.
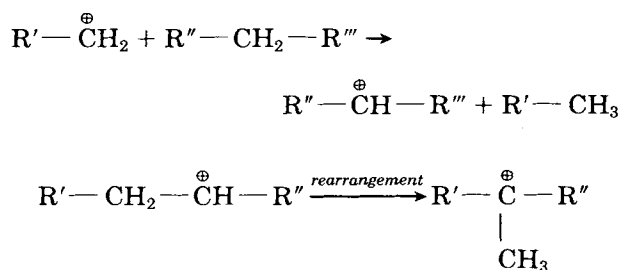
DISCUSSION

Figures 3–5 indicate that C$_4$ alkenes were the most abundant volatile products detected during TGA-MS analysis of the poly(ethylene)/silica-alumina and poly(ethylene)/HZSM-5 samples, and that propene (C$_3$ alkene) was the most abundant volatile product for the poly(ethylene)/sulfated zirconia sample. Pyrolysis-GC/MS results confirmed that the most abundant C$_4$ alkene isomer produced by catalytically cracking poly(ethylene) was isobutene. The carbenium ion model for catalytic cracking[23] can be used to explain the formation of the most abundant volatile products. During
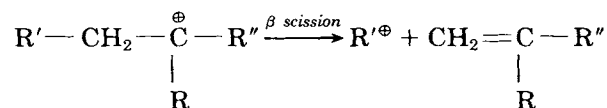
poly(ethylene) cracking, protons from Brönsted acid catalysts can attack polymer chains resulting in chain shortening and the formation of primary carbenium ions.

$$R' - CH_2 - CH_2 - R'' \xrightarrow{H+} R' - \overset{\oplus}{C}H_2 + CH_3 - R''$$
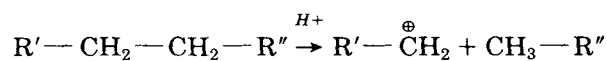
Primary carbenium ions can react via inter- or intramolecular mechanisms to produce secondary carbenium ions, which may rearrange to form more stable tertiary ions.
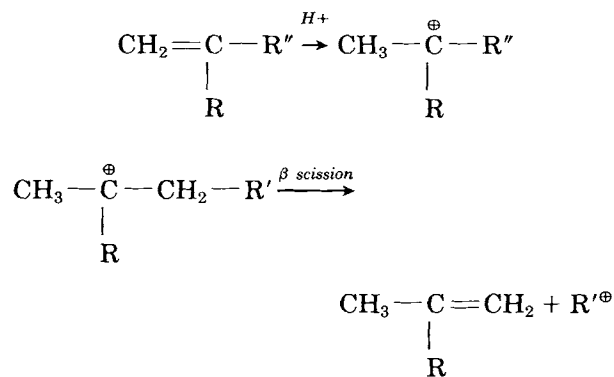
$$R' - \overset{\oplus}{C}H_2 + R'' - CH_2 - R''' \rightarrow$$

$$R'' - \overset{\oplus}{C}H - R''' + R' - CH_3$$

$$R' - CH_2 - \overset{\oplus}{C}H - R'' \xrightarrow{rearrangement} R' - \overset{\oplus}{\underset{\overset{|}{CH_3}}{C}} - R''$$

Beta-scissions of these secondary and tertiary carbenium ions can result in the formation of new primary carbenium ions and chain end olefins.

$$R' - CH_2 - \overset{\oplus}{\underset{\overset{|}{R}}{C}} - R'' \xrightarrow{\beta\ scission} R'^{\oplus} + CH_2 = \overset{}{\underset{\overset{|}{R}}{C}} - R''$$

Chain end olefin double bonds can react with catalyst protons to again form carbenium ions, which, after β-scission, can produce propene or isobutene, depending on whether R in the equation below is H or CH$_3$.

Table V   TGA-MS Class-Specific Activation Energies in kcal/mol

Class	PE/Silica-Alumina	PE/HZSM-5	PE/ZrO$_2$/SO$_4$
Propene	38.30 ± 0.12	33.59 ± 1.67	18.59 ± 0.69
C$_4$-Alkenes	42.69 ± 1.67	29.73 ± 1.06	23.04 ± 1.06
C$_4$-Alkanes	41.60 ± 2.65	25.88 ± 0.14	22.63 ± 0.91
C$_5$-Alkenes	38.75 ± 0.91	29.36 ± 0.94	22.15 ± 0.88
C$_5$-Alkanes	35.75 ± 2.28	27.54 ± 1.68	21.49 ± 1.12
C$_6$-Alkenes	37.94 ± 2.29		23.08 ± 0.50
C$_6$-Alkanes	34.79 ± 3.84		22.18 ± 0.54
C$_7$-Alkenes	33.64 ± 2.75		23.17 ± 0.49
C$_8$-Alkenes	38.27 ± 3.43		23.06 ± 0.63
C$_9$-Alkenes	42.72 ± 1.58		
Aromatics		29.17 ± 0.48	

$$CH_2 = C - R'' \xrightarrow{H^+} CH_3 - \overset{\oplus}{C} - R''$$
$$\qquad | \qquad\qquad\qquad |$$
$$\qquad R \qquad\qquad\qquad R$$

$$CH_3 - \overset{\oplus}{C} - CH_2 - R' \xrightarrow{\beta\ scission}$$
$$\qquad |$$
$$\qquad R$$

$$CH_3 - C = CH_2 + R'^{\oplus}$$
$$\qquad |$$
$$\qquad R$$

The relative abundance of propene in TGA–MS cracking products can be correlated with the catalyst acidity (i.e., sulfated zirconia > HZSM-5 > silica alumina), suggesting that rearrangement of secondary carbenium ions to tertiary ions is less important for high acidity catalysts.

The TGA–MS weight loss curve for the poly(ethylene)/silica-alumina sample (Fig. 2) clearly shows that two steps are involved in volatile product formation for this sample. In fact, class-specific temperature profiles shown in Figures 3–5 show that alkene and alkane production occurred in two steps for all three catalysts. The maximum rate of volatile product formation for the first step occurred at about 320°C for the sample containing the silica-alumina catalyst but at about 200°C for samples containing the higher acidity HZSM-5 and sulfated zirconia catalysts. The maximum rate of volatile product formation for the second step occurred at 425°C for the poly(ethylene)/silica-alumina sample, at 270°C for the poly(ethylene)/HZSM-5 sample, and at 250°C for the poly(ethylene)/sulfated zirconia sample. The general trend was that the rate of product formation in the second stage maximized at lower temperatures for higher acidity catalysts.

Because all three polymer/catalyst samples exhibited two stage cracking mechanisms, the two steps were most likely due to heterogeneity in the poly(ethylene). The first stage of volatile product formation may result from catalyst protons attacking polymer defect groups such as internal or terminal double bonds.[9] The second step may reflect the acid catalyzed cracking of the —CH2— polymer backbone.

Figure 6 and Table II indicate that the HZSM-5 catalyst was particularly effective at forming aromatics. One difference between this catalyst and the others was that HZSM-5 had a crystalline structure containing two intersecting channels.[24] One HZSM-5 channel is straight and has a nearly circular open-

ing (0.54 × 0.56 nm), and the other channel is sinusoidal and somewhat more elliptical (0.51 × 0.56 nm). The acid sites of HZSM-5 are located within these channels. Therefore, acid catalyzed reactions occur within a restricted volume. The fact that aromatics were detected only after significant quantities of alkenes were observed suggests that aromatics were formed by alkene oligomerization reactions. Due to the restricted HZSM-5 channel volume, oligomerization reactions resulted in the efficient formation of small alkyl aromatics.

By comparing the TGA–MS weight loss curve for the poly(ethylene)/sulfated zirconia sample shown in Figure 2 with the hydrocarbon class temperature profiles shown in Figure 5, it can be seen that the weight loss that occurred above 350°C for this sample did not result in the formation of hydrocarbon products. Mass spectra obtained during this high-temperature weight loss step indicated that the primary volatile products were SO_2 and CO_2. Thus, at temperatures above 350°C, the sulfated zirconia catalyst decomposed. However, under identical TGA–MS analysis conditions but in the absence of a polymer, no SO_2 evolution was detected and the sulfated zirconia catalyst was found to be stable to 600°C. Apparently, species formed near the sulfated zirconia acid site during poly(ethylene) cracking were responsible for making the catalyst thermally unstable below 600°C. The TGA–MS temperature profiles for m/z 64 (SO_2) and m/z 44 (CO_2) shown in Figure 7 indicate that SO_2 evolution preceded CO_2 evolution. This is consistent with a sulfated zirconia decomposition mechanism in which SO_2 and oxygen atoms are the initial degradation products.[25] In the absence of adsorbates, individual oxygen atoms eventually combine to produce O_2. However, when organics are present on the catalyst surface, oxygen
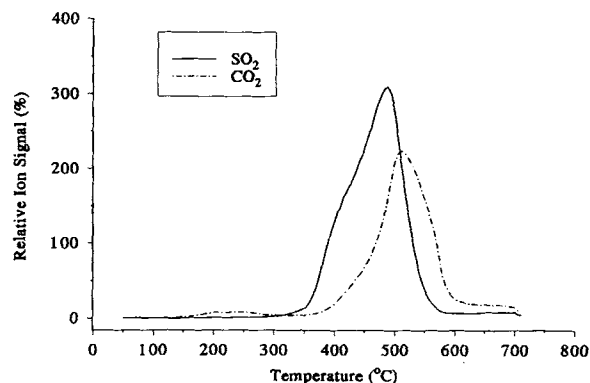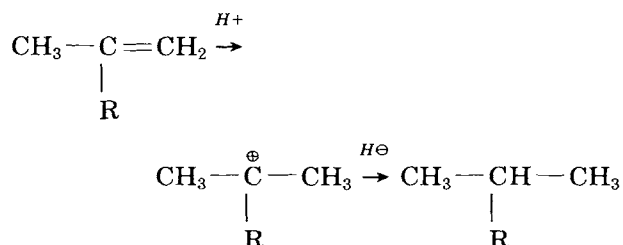

Figure 7   Ion signal temperature profiles for SO_2 (m/z 64) and CO_2 (m/z 44) derived from TGA–MS analysis of the poly(ethylene)/sulfated zirconia sample.

atoms can react to ultimately form CO_2. The fact that CO_2 evolution occurred after SO_2 was detected is indicative of an induction period that would be expected prior to the formation of significant amounts of CO_2.

CONCLUSIONS

The primary products detected in this study are not the same as those previously reported for the catalytic cracking of poly(ethylene).[4-11] The primary low-temperature volatile products reported in previous work were isoalkanes, whereas isoalkenes were the primary products detected in this study. However, the mechanism proposed for isoalkane formation[10] requires the protonation of volatile alkenes followed by hydride abstraction from the polymer residue.

$$CH_3 - \overset{\displaystyle |}{\underset{\displaystyle R}{C}} = CH_2 \xrightarrow{H+}$$

$$CH_3 - \overset{\displaystyle |}{\underset{\displaystyle R}{\overset{\oplus}{C}}} - CH_3 \xrightarrow{H\ominus} CH_3 - \overset{\displaystyle |}{\underset{\displaystyle R}{CH}} - CH_3$$

The fact that little isoalkane production was detected in our study suggests that these reactions were of little importance during TGA–MS thermal analysis and that the analysis method described here can be an effective means to study the effects of catalysts on the initial reactions involved in polymer cracking. However, to achieve a better understanding of polymer catalytic cracking processes, the characterization experiments described here should be coupled with catalytic reactor studies.

REFERENCES

1. *Standard Guide—The Development of Standards Relating to the Proper use of Recycled Plastics,* ASTM Designation D 5033-90, Philadelphia, 1990.
2. W. E. Pearson, *Designing Recycling to Perserve Packaging Innovation,* Packaging Research Foundation, Kennett Square, PA, April 1993.
3. C. Noto la Diega and V. Variali, *Acqua Aria,* **2,** 131 (1982).
4. Y. Uemichi, A. Ayame, Y. Kashiwaya, and H. Kanoh, *J. Chromatogr.,* **259,** 69 (1983).
5. Cr. I. Simionescu, C. Vasile, P. Onu, M. Sabliovschi, G. Moroi, V. Barboiu, D. Ganju, and M. Florea, *Thermochim. Acta,* **134,** 301 (1988).
6. P. L. Beltrame, P. Carniti, G. Audisio, and F. Bertini, *Polym. Degrad. Stab.,* **26,** 209 (1989).
7. Y. Ishihara, H. Nanbu, T. Ikemura, and T. Takesue, *J. Appl. Polym. Sci.,* **38,** 1491 (1989).
8. Y. Ishihara, H. Nanbu, T. Ikemura, and T. Takesue, *Fuel,* **69,** 978 (1990).
9. S. R. Ivanova, E. F. Gumerova, A. A. Berlin, K. S. Minsker, and G. E. Zaikov, *Russ. Chem. Rev.,* **60,** 225 (1991).
10. Y. Ishihara, H. Nanbu, K. Saido, T. Ikemura, and T. Takesue, *Bull. Chem. Soc. Jpn.,* **64,** 3585 (1991).
11. Y. Ishihara, H. Nanbu, K. Saido, T. Ikemura, and T. Takesue, *Polymer,* **33,** 3482 (1992).
12. H. Ohkita, R. Nishiyama, Y. Tochihara, T. Mizushima, N. Kakuta, Y. Morioka, A. Ueno, Y. Namiki, S. Tanifuji, H. Katoh, H. Sunazuka, R. Nakayama, and T. Kuroyanagi, *Ind. Eng. Chem. Res.,* **32,** 3112 (1993).
13. A. R. Songip, T. Masuda, H. Kuwahara, and K. Hashimoto, *Energy Fuels,* **8,** 136 (1994).
14. T. Okuhara, T. Nishimura, H. Watanabe, and M. Misono, *J. Mol. Catal.,* **74,** 247 (1992).
15. K. Tanabe, H. Hatori, and T. Yamaguchi, *Crit. Rev. Surf. Chem.,* **1,** 1 (1990).
16. B. Umansky, J. Englehardt, and K. Hall, *J. Catal.,* **127,** 128 (1991).
17. F. G. Ciapetta and C. J. Plank, in *Catalysis,* Vol. I, P. H. Emmett, Ed., Reinhold, New York, 1954, pp. 341-342.
18. A. Jatia, C. Chang, J. D. MacLeod, T. Okube, and M. E. Davis, *Catal. Lett.,* **25,** 21 (1994).
19. R. L. White, *J. Anal. Appl. Pyr.,* **18,** 269 (1991).
20. T. A. Iida, K. Honda, and H. Nozaki, *Bull. Chem. Soc. Jpn.,* **46,** 1480 (1970).
21. H. L. Friedman, *J. Polym. Sci.,* **6C,** 183 (1963).
22. T. H. Risby and A. L. Yergey, *Anal. Chem.,* **50,** 327A (1978).
23. C. L. Thomas, *Ind. Eng. Chem.,* **41,** 2564 (1949).
24. G. T. Kokotailo, S. L. Lawton, D. H. Olson, and W. M. Meier, *Nature,* **272,** 437 (1978).
25. S. Chokkaram, R. Srinivasan, D. R. Milburn, and B. H. Davis, *J. Colloid Interface Sci.,* **165,** 160 (1994).